Sustainable Energy & Fuels

ROYAL SOCIETY OF CHEMISTRY

PAPER

View Article Online
View Journal | View Issue

Cite this: *Sustainable Energy Fuels*, 2025, **9**, 2119

Optimization and characterization of biocrude produced from hydrothermal liquefaction of food waste

Kshanaprava Dhalsamant and Ajay K. Dalai *

This study investigates the valorization of restaurant-derived food waste into biocrude using hydrothermal liquefaction (HTL). The selected feedstocks, including carrot, parsnip, and other vegetables, were evaluated for their physicochemical properties, showing low ash (9.1–22.0 wt%) and fixed carbon content (5.3–18.4 wt%) with high moisture levels (79–95% wet basis), suitable for HTL without additional drying. Carrot emerged as the optimal feedstock due to its elevated carbon (44.9 wt%), hydrogen (7.8 wt%), cellulose (15.3 wt%), and hemicellulose (4.1 wt%) content. Reaction parameters optimized *via* response surface methodology (280 °C, 1500 psi, 42 minutes) yielded 18.8 wt% biocrude with a carbon recovery of 55.9–72.8%. Quality analyses such as gas chromatography-mass spectrometry and Fourier-transform infrared spectroscopy highlighted the complex composition of biocrude, including esters, hydrocarbons, and oxygenated compounds, confirming its potential for biofuel applications. Solvent optimization experiments demonstrated that methanol was the most effective, yielding 19.6 wt% biocrude. Additionally, methanol actively participated in the extraction process by promoting esterification, generating methyl esters, as evidenced in gas chromatography-mass spectrometry analysis. These reactions enhance product yield and quality by forming bioactive compounds like methyl esters, which improve the bio-oil stability and calorific value. Despite high oxygen content (20.7 wt%), the biocrude properties can be upgraded *via* deoxygenation techniques, paving the way for its use as a sustainable transportation fuel. This research underscores hydrothermal liquefaction as an effective approach to manage food waste while addressing global energy challenges through renewable bioenergy production. By integrating statistical optimization and comprehensive characterization, this study contributes to advancing biofuel technology and sustainable energy solutions.

Received 29th January 2025
Accepted 17th February 2025

DOI: 10.1039/d5se00136f

rsc.li/sustainable-energy

1. Introduction

In 2018, the overall output of fruits and vegetables in Canada amounted to 3 048 143 metric tons, with a corresponding food waste of 90 600 tons (~3%).[1] The production of fruits and vegetables in Canada experienced a notable increase, reaching a total of 3 208 388 metric tons in the year 2022.[2] Consequently, it is expected that the amount of food waste has also risen in recent years, aligning with previous trends and the growth of the population. The statistics of fruit and vegetable production and waste in Canada are given in Tables 1 and 2. Furthermore, the category of food waste includes residual food products within the food industry, restaurants, and kitchens, as well as rotten food items originating from grocery stores or landfills. This form of waste significantly contributes to the phenomenon of global warming through the emission of greenhouse gases. Food waste (FW) refers to food that has not fulfilled its intended function.[3,4] The phenomenon of global food waste is exhibiting a concurrent rise with the growth of the global population and the escalation of food consumption.[5] In recent times, there has been a growing international focus on energy security, environmental sustainability, and the increasing output of waste. As a result, there has been a notable increase in research endeavors aimed at discovering alternative and renewable energy sources. Food waste affects food security and the economy of a country by affecting the improper use of investment and nutrition. Therefore, the utilization of food waste to produce biofuels as a means of generating green energy presents an alternative strategy for addressing the challenges. An area that is currently receiving significant attention is the process of valorizing food waste, which is a widespread problem that has extensive economic, environmental, and social consequences.[5] Food waste not only places a burden on landfills and contributes to the release of greenhouse gases, but it also results in the wastage of valuable resources that are inherent within it. Simultaneously, the transportation industry continues to largely depend on fossil fuels, hence intensifying the depletion

Catalysis and Chemical Reaction Engineering Laboratories, Department of Chemical and Biological Engineering, College of Engineering, University of Saskatchewan, Saskatoon, SK, Canada S7N 5A9. E-mail: akd983@mail.usask.ca; Tel: +1-306-546-0742

Table 1 Canada statistics on fruit and vegetable production[2]

	Vegetables	Fruits	Western Canada vegetables			
Rank	Canada (metric ton)	Canada (metric ton)	Manitoba (ton)	Saskatchewan (ton)	Alberta (ton)	British Columbia (ton)
1	Tomato (528 938)	Apple (414 494)	Carrot (6842)	Cabbage (1474)	Onion (30 806)	Cabbage (8793)
2	Carrot (348 135)	Cranberry (228 565)	Onion (4562)	Carrot (1076)	Sweet corn (13 932)	Carrot (7552)
3	Onion (287 499)	Blueberry (195 892)	Cabbage (3172)	Pumpkin (341)	Pumpkin (4463)	Sweet corn (6865)
4	Sweet corn (201 028)	Grape (98 116)	Cauliflower (2775)	Sweet corn (156)	Cabbage (4377)	Pumpkin (6727)

Table 2 Canada statistics on food production waste[1]

Year	Production (metric ton)	Loss (ton)	Year	Production (metric ton)	Loss (ton)
2011	2 916 296	51 358	2017	—	—
2012	2 968 533	49 758	2018	3 138 185	90 600
2013	2 991 266	51 273	2019	3 160 390	—
2014	3 027 260	83 130	2020	3 089 499	—
2015	3 048 398	87 415	2021	3 074 509	—
2016	3 268 389	88 415	2022	3 208 388	—

of limited resources and aggravating environmental issues. The utilization of biofuel obtained from biomass has promising prospects as a feasible cornerstone for the establishment of sustainable energy sources.[6]

In response to these interconnected issues, there has been an increasing focus on the conversion of food waste into biocrude, a versatile intermediary substance that has the potential to function as a sustainable substitute for traditional transportation fuels.[7,8] Biocrude, which is derived from the hydrothermal liquefaction (HTL) process, offers a potential answer by facilitating the recycling of biological waste materials and the production of sustainable energy sources.[9] Generally, HTL is preferred for biocrude production from food waste as it uses the water already present in the food, therefore it does not need drying of feedstock prior to reaction.[5,10] This study undertakes a thorough investigation into the process of converting food waste into biocrude and evaluates its potential as a viable transportation fuel through further characterization.

The biochemical content of food waste has a considerable influence on the results of HTL. The presence of a large amount of lipids in food waste increases the liquid yield in the HTL process, which in turn leads to higher production of biocrude.[5] The protein and carbohydrate levels of a product also influence its quality, as they affect the composition of the biocrude and biochar product. Carbohydrate rich biomass leads to low biocrude yield, and high biochar yield.[11] Protein rich feedstocks give high ammonia content in the aqueous phase. The formation of amines from proteins occurs at lower temperatures, which accounts for the increased biocrude production from beef at lower temperatures of 280–300 °C.[12] Most of the biocrude derived from chicken is produced by the Maillard process, which is more favorable at elevated temperatures of 280–360 °C.[13] Gaining a comprehensive understanding of these complex interactions is essential for maximizing the efficiency of HTL operations and achieving optimal conversion of food waste into useful bioenergy resources.[5,11] This research not only tackles waste management concerns but also supports the overarching objective of sustainable energy production by utilizing various biomass feedstocks.

A study used hydrothermal carbonization (HTC) and HTL on an industrial feedstock with a moisture content of 53 wt%, including sweeteners, nuts, eggs, fish products, dairy products, meat, poultry, fresh and processed vegetables and fruits, and grain products.[14] Elevated temperatures diminish liquid production, increase gas generation, and decrease charcoal formation. However, biochar carbonization rises with temperature. According to Pecchi *et al.*,[14] lipid hydrolysis begins at 220 °C but accelerates at temperatures above 250 °C. Thus, a low-temperature HTL process reduces energy consumption, enabling full lipid breakdown and long-chain fatty acid conversion.

Anaerobic digestion (AD) and composting are carried out for conversion of food wastes for biomethane and fertilizer, respectively.[15,16] However, the benefits of HTL compared to AD are notably reduced processing duration (days/weeks *versus* minutes/hours), decreased reactor size, and rapid initiation period. This process is useful for liquid fuels and biochar production. HTL obviates the expensive prerequisites for pretreatment, in contrast to AD.[17]

Statistical and mathematical optimization techniques, like the Response Surface Method (RSM), have been employed to optimize the response parameters in HTL.[18] RSM is a robust statistical technique used to fit multiple regression models to output data obtained from a simulation model. Its primary objective is to determine the optimal parameter settings that yield the best results. This method is commonly employed in situations where various independent variables influence dependent variables. For example, Xu *et al.*[19] investigated how various operating parameters affected the HTL of sewage waste

from municipal areas and reported that temperature is the most important process factor in the HTL process.

The conversion of biocrude from food waste serves the dual purpose of resolving waste management challenges and responding to the pressing demand for cleaner energy alternatives. The adoption of this comprehensive strategy has the potential to make a substantial impact on the mitigation of carbon emissions, mitigation of strain on waste disposal sites, and establishment of sustainable energy routes. Nevertheless, to effectively incorporate biocrude into the transportation industry, it is imperative to possess a comprehensive understanding of its chemical composition, physicochemical features, and combustion attributes. The objective of this study is to address the existing gap in knowledge by providing a comprehensive understanding of the potential of biocrude as a sustainable and environmentally friendly fuel for transportation purposes.

In the forthcoming sections of this scholarly article, we will explore the approaches utilized in the generation of biocrude from food waste *via* the process of HTL. Additionally, a comprehensive examination will be conducted on the physicochemical characteristics of the biocrude that is generated, with particular emphasis on its suitability as a fuel for transportation purposes. The anticipated results of this study are poised to make valuable contributions to the scholarly discourse surrounding bioenergy and waste valorization. Additionally, they are expected to provide valuable insights to policymakers and stakeholders regarding the potential advantages and obstacles entailed in the integration of biocrude into the current transportation infrastructure.

The novelty of this study is related to the HTL of food waste for a high biocrude yield by optimizing reaction parameters. In addition to thorough screening of food waste to produce high yields of biocrude using HTL technology, the RSM technique was used to bring out the different combinations of reaction parameters for finding out the important parameters affecting biocrude production. Additionally, an optimization study of solvent identification and recovery was undertaken by using various solvents for filtration to yield a higher quality of biocrude. The solvent selection was based on the solvents with low to high polarity (methanol, acetone, ethyl acetate, ethanol, dichloromethane, toluene, and hexane). Studying the impact of different solvents on the process allows for the optimization of product yield and quality, providing novelty on the sustainable production of bio-crude from food waste using customized HTL techniques. Additionally, different quality analyses (gas chromatography-mass spectrometry (GC-MS) and inductively coupled plasma-optical emission spectrometry (ICP-OES) techniques) were performed with new analytical tools to gain an in-depth understanding of the biocrude properties including composition. The outcomes of this study have the potential to not only redefine the discourse surrounding sustainable waste management but also accelerate the transition towards cleaner and more sustainable energy sources within the transportation industry.

2. Materials and methods

2.1. Feedstocks and chemicals

The feedstock utilized for HTL reactions in this investigation consisted of food waste obtained from the restaurant located at the University of Saskatchewan in Saskatoon, Canada. The feedstock obtained as food wastes included beetroot, brussels sprouts, cabbage, carrot, celery, corn, onion, parsnip, pumpkin, and tomato. The samples were collected, sorted, and made into a slurry with the help of an industrial grinder (Cgoldenwall, 2500 W, Canada).

2.2. Feedstock characterization

For the proximate analysis of the samples, the moisture content of the fresh food wastes was estimated by the ASTM D3137 method. Similarly, the volatile matter content and ash of the dry mass were calculated by the ASTM D3175 and D3174 methods, respectively. The volatile matter content was calculated from eqn (1), and the fixed carbon content was determined by the method of subtraction as given in eqn (2).

$$\text{Volatile matter content (wt\%)} = \frac{[(\text{mass of oven dried sample} - \text{mass of residue}) - \text{mass of residual moisture in oven dried sample}]}{\text{mass of oven dried sample}} \quad (1)$$

$$\text{fixed carbon content (wt\%)} = 100 - [\text{moisture content (wt\%)} + \text{ash content (wt\%)} + \text{volatile] matter content (wt\%)} \quad (2)$$

The modified Van Soest method was employed for detergent fibre analysis using an Ankom 200 Fibre Analyzer (ANKOM Technology, Macedon, NY). The acid detergent lignin (ADL), acid detergent fiber (ADF), and neutral detergent fiber (NDF) data were collected using the Ankom 200 Method, 8, 5, and 6 respectively.[20] The extraction of fibre components, such as lignin, cellulose, hemicellulose, ash, and extractives, was performed using NDF, ADF, and ADL solutions.[7] The examination of food wastes' bio-composition was conducted in two sequential processes. The initial stage involved the separation of the extractives from the biomass through a series of solvent extractions utilizing hexane, ethanol, and water in a Soxhlet system. During the second phase, the biomass stripped of extractives was examined to determine its fibre (or polysaccharide) and lignin composition.[21] The biomass was subjected to gravimetric analysis using the Van Soest method to

determine the quantities of cellulose, hemicellulose, and lignin. In this procedure, the preliminary estimation of NDF, which consists of cellulose, hemicellulose, and lignin, was conducted by combining 1 g of biomass with 100 mL of a neutral detergent solution, 0.5 g of sodium sulfite, and 1 g alpha-amylase in a round bottom flask and the mixture was then refluxed for 1 hour. For making 1 liter of neutral detergent solution, distilled water (0.99 L), sodium lauryl sulfate (30 g), ethylenediaminetetraacetic acid (EDTA) disodium salt (18.61 g), sodium borate decahydrate ($Na_2B_4O_7 \cdot 10H_2O$) (reagent grade) (6.81 g), sodium phosphate dibasic (Na_2HPO_4) anhydrous (reagent grade) (4.56 g), and triethylene glycol (reagent grade) (10 ml) were mixed. From this mixture of neutral detergent, 100 ml was taken for analysis. Following the reflux process, the reaction mixture was passed through a pre-weighed crucible employing filtration. The crucible containing the NDF was placed in a hot air oven at 105 °C for 8 hours. Upon reaching a lower temperature, the crucible was measured in terms of weight, and the NDF was determined using the subsequent equations (eqn (3)–(8)):

$$\text{NDF (wt\%)} = \frac{(\text{weight of crucible} + \text{NDF}) - \text{weight of crucible}}{\text{weight of biomass}} \times 100 \quad (3)$$

To estimate the ADF, the solid residue obtained from the NDF analysis was treated with an acid detergent solution consisting of 20 g cetrimonium bromide in 1000 mL of 1 N H_2SO_4. The mixture was then heated under reflux for 1 hour. Following the completion of the ADF estimating process, the response was halted. The ADF mixture underwent filtration, and then was transferred into a crucible and subjected to drying at 105 °C for 8 hours. The ADF was computed using the subsequent formula:

$$\text{ADF (wt\%)} = \frac{(\text{weight of crucible} + \text{ADF}) - \text{weight of crucible}}{\text{weight of biomass}} \times 100 \quad (4)$$

$$\text{hemicellulose (wt\%)} = \text{NDF (wt\%)} - \text{ADF (wt\%)} \quad (5)$$

$$\text{cellulose (wt\%)} = \frac{(\text{weight of crucible} + \text{ADF}) - (\text{weight of crucible} + \text{lignin})}{\text{weight of biomass}} \times 100 \quad (6)$$

$$\text{lignin (wt\%)} = \frac{(\text{weight of crucible} + \text{lignin}) - (\text{weight of crucible} + \text{ash})}{\text{weight of biomass}} \times 100 \quad (7)$$

$$\text{extractives (wt\%)} = 100 - [\text{cellulose (wt\%)} + \text{hemicellose (wt\%)} + \text{lignin (wt\%)} + \text{ash (wt\%)}] \quad (8)$$

A CHNSO analyzer (PerkinElmer Elementar, Vario EL III, Elementar Americas Inc., NJ) was utilized to conduct the ultimate analysis. The final composition, comprising carbon (C), hydrogen (H), nitrogen (N), and sulphur (S), was determined, while the oxygen content was determined by difference.

2.3. Hydrothermal liquefaction conversion in the reactor system

The food waste paste was used as feedstock for the HTL reactor as shown in Fig. 1. 500 g of feedstock was placed in a 1 L reactor (4848, PARR Instrument Company, US), at different sets of temperature, pressure, and time at 550 rpm rotor speed. The inherent moisture present in the feedstocks served as the reaction medium during the hydrothermal liquefaction (HTL) process, with no additional water added. The experiments were conducted under hydrothermal conditions facilitating thermochemical reactions such as hydrolysis and depolymerization. These conditions align with the standard criteria for HTL, where water acts as a reaction medium, solvent, and catalyst. These results confirm the hydrothermal nature of the process and distinguish it from simple liquefaction.

Following the conclusion of the reaction, the reactor underwent a cooling process, and the slurry from the reactor was vacuum filtered for separating the aqueous phase from the biochar + biocrude mixture. Then the biochar + biocrude mixture was treated with acetone solvent (Fisher Scientific, Edmonton, Canada) with a 1 : 10 ratio and heated to extract the biocrude from the biocrude + biochar mix. After the heat treatment, the mixture was vacuum filtered to separate the biochar from the biocrude + solvent mix. Further, acetone was separated from the biocrude using a rotary evaporator (BUCHI Waterbath, B-480, Switzerland). The process flow of production of biocrude from the feedstock is given in Fig. 2.

2.4. Design of experiments

The Design-Expert program (version 11.0) was utilized to conduct the tests with a superior design. The Central Composite Design (CCD) procedure was applied to construct the experiments aimed at optimizing process parameters, including temperature (ranging from 280 to 320 °C), pressure (ranging from 1500 to 1900 psi), and reaction time (spanning from 15 to 45 minutes). The present study investigates the impact of these parameters on the biocrude yield (%) and oxygen content (%) of the biocrude during HTL reaction. To examine the individual and combined effects of these parameters, a series of

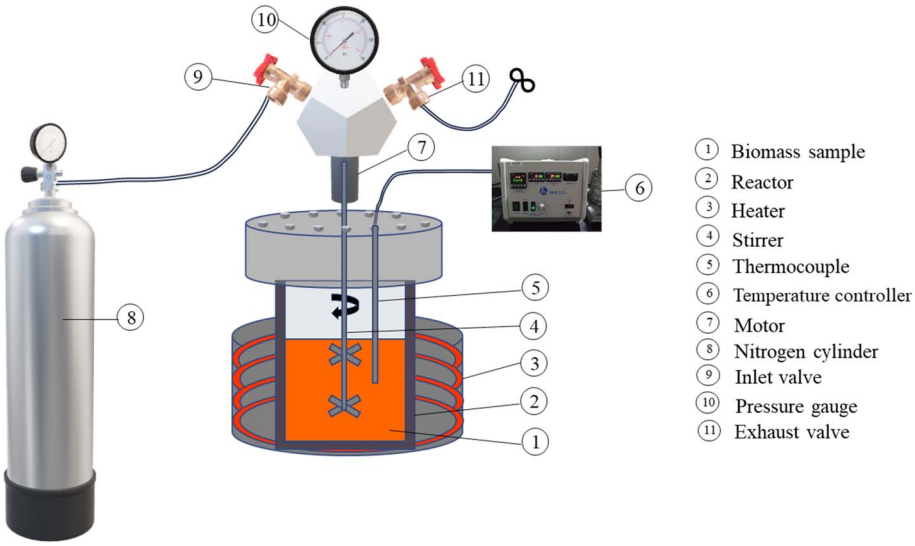

Fig. 1 Schematic representation of the experimental run in HTL with the feedstock.

experiments were conducted using CCD. The dependability of the model is contingent upon several factors, including *F*-test value, *p*-value, adjusted R^2, R^2, and forecasted R^2. The experiments were conducted in duplicate. The number of tests for the CCD and biocrude yield was calculated from eqn (9) (ref. 22) and eqn (10),[23] respectively. The oxygen content was obtained from the elemental analysis of the biocrude.

$$N = 2^n + 2n + k \quad (9)$$

where n is the number of parameters, and k is the number of axial points, usually 6.

Similarly, the biocrude yield was obtained from eqn (8).

$$\text{Biocrude yield} = \frac{M_{\text{biocrude}}}{M_{\text{feedstock}}} \times 100 \quad (10)$$

where M_{biocrude} is the mass of biocrude obtained after HTL reaction, and $M_{\text{feedstock}}$ is the mass of dry matter of the feedstock.

2.5. Quality analyses

2.5.1. Higher heating values. The higher heating value (HHV) in MJ kg^{-1} of the feedstock and biocrude was determined by employing an oxygen bomb calorimeter (PARR 6400 Calorimeter, IL, USA) in accordance with the ASTM D5865 standard. The viscosity of the biocrude was determined at a temperature of 40 °C using the Brookfield DV-I viscometer (CAN-AM Instruments Ltd, Ontario, Canada).

2.5.2. Thermogravimetric analysis. The devolatilization features of the biomasses were assessed using thermogravimetric analysis (TGA) on a PerkinElmer Pyris Diamond TG/DTA instrument (PerkinElmer, USA). A biomass sample weighing 0.5 g was exposed to a temperature program ranging from 25 to 600 °C, with a heating rate of 10 °C per minute. The purge gas utilized in the experiment was argon, which was supplied at a flow rate of 10 mL min^{-1}. The temperature at which HTL tests were conducted was determined by measuring the rate of weight loss in relation to temperature.

2.5.3. Chemical composition. The Fourier-transform infrared spectra (FTIR) of the feedstock and biocrude were acquired utilizing a Bruker Vertex 70 spectrometer (Bruker Corporation, Billerica, MA, USA). The spectrometer employed a collection approach for infrared-spectra using a diamond ATR (attenuated total reflection) crystal. The instrument's spectral-resolution was configured to 8 cm^{-1}, and the recorded spectra encompassed the wavelength range of 4000–400 cm^{-1}.

2.5.4. Gas chromatography-mass spectrometry (GC-MS). The liquid products derived from the HTL of carrot waste were

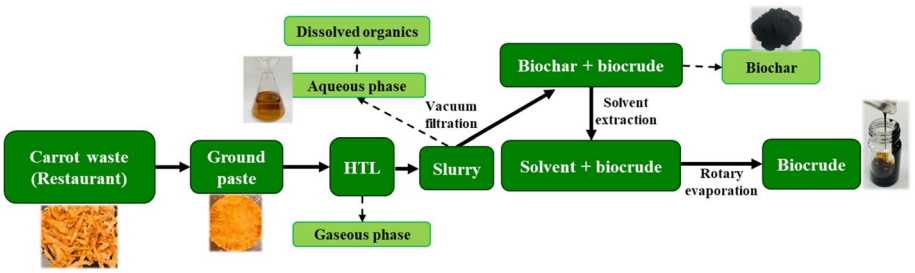

Fig. 2 Flow chart of different steps involved in the conversion of food waste into biocrude through hydrothermal liquefaction (HTL).

subjected to analysis using a gas chromatography-mass spectrometry (GC-MS, Agilent Technologies, 7890A, JEOL, Agilent, Canada) instrument. This analysis aimed to identify and quantify the chemical constituents present in the liquid products after filtration using various solvents. The quantitative analysis of biocrude components was performed by comparing the peak area of the internal standard discovered by the Flame Ionization Detector (FID). Perfluorotributylamine was employed for calibrating the mass spectrometer in the study. The capillary column employed in this study was a DB-5 MS (30 m × 0.25 mm × 0.25 μm, Agilent, USA). The temperature of the injector was held constant at 275 °C. The oven temperature was set to increase from 40 to 320 °C at a heating rate of 15 °C per minute. The temperature was maintained at 40 °C for a duration of 5 minutes, and at 320 °C for a duration of 10 minutes. The temperature was subsequently raised to 250 °C and maintained for a duration of 2 minutes. The carrier gas utilized in this study was helium of chromatographic quality, with a flow-rate of 0.2 mL min^{-1}. The mass range (m/z) of the mass spectrometer was configured to span from 30 to 700. The identification of the chemicals was conducted by utilizing the National Institute of Standards and Technology (NIST) mass spectrum database included in the TSS Unity software.

2.5.5. Mineral compositions. The mineral compositions of biocrude were analyzed using an inductively coupled plasma-optical emission spectrometry (ICP-OES) technique (iCAP 7000 Series, Thermoscientific, Canada) instrument. Aqua regia as acidic digestates were acquired by employing a combination of concentrated hydrochloric acid (HCl) and nitric acid (HNO_3) in a 4 : 1 (v/v) ratio.

3. Results and discussion

The physicochemical analysis of the food wastes was analyzed as discussed in the Materials and methods. The proximate analysis of the samples is given in Table 3, and the fiber and ultimate analysis of the feedstock is shown in Table 4.

As can be seen from Table 3, the food wastes collected from restaurants have a high moisture content, which serves as the reaction medium for the hydrothermal liquefaction of the food wastes. However, the feedstock for the HTL reaction was chosen based on the vegetable having low ash content, and low fixed carbon content as the focus is to get high biocrude yield.[24] Similarly, feedstocks having high lignin, cellulose, carbon, and hydrogen content were preferred for the HTL reaction as they contribute towards the high biocrude yield.[25] As can be seen from the fiber and ultimate analysis from Table 4, the carbon and hydrogen contents in carrots are higher than the rest of the vegetables, therefore, carrots was chosen as the feedstock for HTL.[26] However, each vegetable analyzed in this study has the potential to produce biocrude to some extent, which will be accessed in future studies.

Table 3 Proximate analysis of food wastes

Food wastes	Moisture content (% wt, fresh)	Moisture content (wt%, oven dried)	Ash content (wt%)	Volatile matter content (wt%)	Fixed carbon content (wt%)
Beetroot	86.0 ± 0.2	0.9 ± 0.1	10.1 ± 0.7	77.6 ± 0.8	11.4 ± 0.1
Brussels sprout	82.0 ± 0.1	0.6 ± 0.1	22.0 ± 0.6	69.4 ± 0.9	8.0 ± 0.4
Cabbage	90.8 ± 0.2	1.3 ± 0.3	18.2 ± 0.3	68.7 ± 0.3	11.8 ± 0.6
Carrot	90.0 ± 0.3	0.4 ± 0.0	9.7 ± 0.9	84.6 ± 0.3	5.3 ± 0.3
Celery	93.0 ± 0.7	0.5 ± 0.1	12.6 ± 0.9	79.3 ± 0.9	7.6 ± 0.5
Corn	79.5 ± 0.4	1.2 ± 0.1	9.8 ± 0.8	72.0 ± 0.7	17.0 ± 0.3
Onion	89.4 ± 0.3	1.4 ± 0.4	10.1 ± 0.7	79.6 ± 0.8	9.0 ± 0.7
Parsnip	80.0 ± 0.3	0.8 ± 0.0	9.8 ± 0.7	74.8 ± 0.3	14.7 ± 0.9
Pumpkin	79.0 ± 0.1	0.6 ± 0.1	10.4 ± 0.2	79.4 ± 0.6	9.6 ± 0.2
Tomato	95.4 ± 0.3	1.1 ± 0.2	9.1 ± 0.2	71.3 ± 0.8	18.4 ± 0.1

Table 4 Fiber and ultimate analysis of food wastes

Food waste (dry basis)	Fiber analysis				C (wt%)	H (wt%)	N (wt%)	S (wt%)	Ash (wt%)	O (wt%)
	Lignin (wt%)	Cellulose (wt%)	Hemicellulose (wt%)	Extractives (wt%)						
Beetroot	7.0 ± 0.7	8.4 ± 0.5	13.1 ± 0.1	61.4 ± 0.3	42.6	5.6	2.4	0.2	10.0	39.1
Brussels sprout	5.7 ± 0.0	11.7 ± 0.4	7.6 ± 0.3	53.0 ± 0.6	41.2	6.0	4.7	0.7	22.0	25.4
Cabbage	5.2 ± 0.2	12.4 ± 0.4	2.4 ± 0.1	61.8 ± 0.2	41.6	5.7	2.1	0.6	18.2	31.7
Carrot	8.1 ± 0.2	15.3 ± 0.2	4.1 ± 0.3	62.8 ± 0.1	44.9	7.8	1.0	0.1	9.7	36.5
Celery	7.7 ± 0.1	11.5 ± 0.3	5.0 ± 0.4	63.2 ± 0.1	42.3	5.7	4.3	0.4	12.6	34.7
Corn	7.9 ± 0.2	5.6 ± 0.3	21.2 ± 0.3	55.4 ± 0.1	42.6	7.4	2.1	0.1	9.8	38.0
Onion	3.8 ± 0.1	6.0 ± 0.1	1.7 ± 0.2	78.4 ± 0.1	42.5	6.4	1.0	0.5	10.1	39.5
Parsnip	8.2 ± 0.2	11.9 ± 0.3	0.5 ± 0.2	69.7 ± 0.1	43.1	5.7	1.6	0.3	9.8	39.6
Pumpkin	10.6 ± 0.1	18.6 ± 0.3	5.9 ± 0.7	54.5 ± 0.1	41.7	6.3	2.7	0.3	10.4	38.7
Tomato	10.1 ± 0.1	11.5 ± 0.2	3.3 ± 0.3	66.0 ± 0.1	41.5	5.5	2.2	0.2	9.1	41.5

3.1. Mass balance of hydrothermal liquefaction of food waste

A set of 20 experimental runs were conducted based on the design model as shown in Table 5. A mass balance was carried out for the 20 runs of experiments, and it was observed that the maximum amount of biocrude (18.8 wt%) and lowest biochar yield (21.6 wt%) were for the reaction parameters 280 °C, 1500 psi, and 45 minutes. The oxygen content of the biocrude was in the range of 11.1–23.3 wt%, showing the need for upgradation.[27,28]

3.2. Statistical analysis of the model

According to the preceding description, a total of twenty sets of experiments were carried out, and the replies were evaluated with regards to the acceptability of the regression model based on various coefficients. The optimization of the process variables was conducted using the reaction model generated by the Design-Expert program. The experimental data was analyzed using various models, including two-factor interaction, linear, quadratic, and cubic models, in order to determine the regression equation. This study examines the correlation between biocrude yields and oxygen content in response to several experimental parameters, including temperature, pressure, and reaction time. The rationality of the model was determined using mathematical properties such as the sequential model sum of squares and the model summary.[29,30]

As previously mentioned in the preceding paragraph, the verification of the model's appropriateness was conducted by examining the model summary statistics, which are provided in Table 6. The comparison between the biocrude yields and oxygen content predicted by the obtained regression model and the corresponding experimental values is presented in Table 5. The acceptability of the statistical model was significantly influenced by two criteria, namely a high *F*-test value and a low *p*-value (probability value), as indicated in Table 7.[31,32] The *F*-test value from Table 7 was found to be 118.8 for biocrude yield, and 40.4 for oxygen content, whereas the *p*-value was <0.0001 for both of them, which evidenced the significant acceptability of the model. A model is considered statistically significant when the *p*-value is less than 0.05 and the *F*-test value is higher. Another crucial factor considered in assessing the quality of the model was the presence of a lack of fit. In a regression model, it is imperative for the lack of fit to be statistically small in order to deem the model acceptable.[33] In the present study, the calculated *p*-values for the model were determined to be 0.06 and 0.07, indicating statistical significance. It is important to acknowledge that in the context of lack of fit, the *p*-value should exceed 0.05.

The impact of model summary statistics (Table 6) on the adequacy of the mathematical model is considerable, as it is influenced by the values of R^2 (coefficient of determination), anticipated R^2, and adjusted R^2.[31,32] According to the table, the quadratic model and two-factor interactive model were suitable for biocrude yield and oxygen content, respectively under the attained experimental results. There was a notable concurrence observed between the adjusted R^2 values (0.9, 0.9) and the corresponding anticipated R^2 values (0.9, 0.9). There is minute difference between the two values when considering significant numbers (<0.02 and <0.04, respectively). Therefore, based on the aforementioned features such as the R^2 values, *F*-test value, and *p*-value, it can be concluded that the regression model developed for the present experiments has a high level of significance and may be regarded as one of the most robust

Table 5 Biocrude yield and oxygen content obtained from hydrothermal liquefaction of carrot wastes designed by Central Composite Design

	Factor 1	Factor 2	Factor 3	Mass balance				
Run	Temperature (°C)	Pressure (psi)	Time (min)	Biocrude yield (wt%) (response 1)	Aqueous phase (wt%)	Biochar (wt%)	Gas (wt%)	Oxygen content (wt%) (response 2)
1	280	1700	30	17.8	2.8	26.6	52.8	19.3
2	320	1500	15	14.6	1.9	33.0	50.5	14.3
3	320	1900	15	14.2	2.3	32.6	50.9	11.1
4	300	1700	30	16.0	2.6	30.6	50.8	15.3
5	300	1700	30	16.2	2.8	32.2	48.8	16.3
6	300	1900	30	15.4	2.2	32.4	50.0	16.1
7	280	1500	45	18.8	2.8	21.6	56.8	17.7
8	300	1700	30	16.4	2.2	32.8	48.6	16.1
9	280	1900	45	18.4	2.7	23.8	55.1	23.3
10	300	1700	30	16.6	2.8	32.8	47.8	15.5
11	280	1500	15	16.6	2.8	25.6	55.0	17.5
12	320	1900	45	14.6	2.8	32.0	50.6	15.2
13	300	1500	30	16.4	2.9	29.4	51.3	16.2
14	300	1700	30	16.2	2.8	31.6	49.4	15.3
15	320	1500	45	14.8	2.7	34.8	47.7	12.2
16	300	1700	45	15.6	2.5	29.4	52.5	18.5
17	320	1700	30	14.6	2.3	34.0	49.1	13.7
18	280	1900	15	16.2	2.3	28.4	53.1	18.3
19	300	1700	15	14.6	2.4	29.8	53.2	16.1
20	300	1700	30	16.2	2.6	31.8	49.4	15.7

Table 6 Model summary statistics

Source	Sequential p-value	Std. dev.	Lack of fit p-value	R^2	Adjusted R^2	Predicted R^2	Remark
Response 1: biocrude yield							
Linear	<0.0001	0.471	0.001	0.881	0.858	0.773	
2FI	0.0160	0.356	0.002	0.945	0.919	0.922	
Quadratic	**0.0003**	**0.166**	**0.057**	**0.991**	**0.982**	**0.962**	**Suggested**
Cubic	0.9531	0.204	0.006	0.992	0.973	−7.317	Aliased
Response 2: oxygen content							
Linear	<0.0001	1.3300	0.004	0.788	0.738	0.529	
2FI	**0.0002**	**0.7110**	**0.070**	**0.949**	**0.926**	**0.886**	**Suggested**
Quadratic	0.3735	0.6984	0.061	0.962	0.928	0.787	
Cubic	0.6196	0.7445	0.014	0.974	0.919	−22.266	Aliased

mathematical models. Following the assessment of the model's importance, a regression equation was derived and presented in eqn (11) and (12). To assess the validity of the equation, two experimental trials were conducted using randomly selected values for temperature, pressure, and reaction time. Moreover, the biocrude yield and oxygen content, as determined through experimental estimation, exhibited a satisfactory level of concurrence with the anticipated value.

$$\text{Biocrude yield (\%)} = +65.71 - 0.34T - 0.007P + 0.34t + 3.13 \times 10^{-6}TP - 0.0008Tt + 4.17 \times 10^{-6}Pt + 0.0005T^2 + 1.6 \times 10^{-6}P^2 - 0.0015t^2 \quad (11)$$

$$\text{Oxygen content (\%)} = -40.37 + 0.24T + 0.05P - 0.33t - 0.0002TP - 0.001Tt + 0.0005Pt \quad (12)$$

A further crucial component of the model pertains to the examination of variance, commonly referred to as analysis of variance (ANOVA), as demonstrated in Table 7. The ANOVA test table encompasses various statistical terminology, including the F-test value, p-value, degree of freedom, and sum of squares, which have been previously elucidated. The independent variables in the model are deemed significant if $P \leq 0.05$. A higher F value suggests that the variables or model have a stronger statistical significance.[34] The regression model in Table 7

Table 7 Analysis of variance (ANOVA) for process parameters of hydrothermal liquefaction (HTL) of carrot waste

Source	Sum of squares	Degree of freedom	Mean square	F-Value	p-Value	Remark
Response 1: biocrude yield (ANOVA for the quadratic model)						
Model	29.47	9	3.27	118.79	<0.0001	Significant
A: temperature (°C)	21.90	1	21.90	794.74	<0.0001	
B: pressure (psi)	0.44	1	0.44	16.00	0.0025	
C: time (min)	3.84	1	3.84	139.47	<0.0001	
AB	0.0012	1	0.0012	0.05	0.8356	
AC	1.90	1	1.90	68.98	<0.0001	
BC	0.0012	1	0.0012	0.05	0.8356	
A^2	0.47	1	0.47	17.07	0.0020	
B^2	0.07	1	0.07	2.67	0.1332	
C^2	1.30	1	1.30	47.00	<0.0001	
Residual	0.28	10	0.03			
Lack of fit	0.23	5	0.05	4.70	0.0573	Not significant
Pure error	0.05	5	0.01			
Corrected total	29.74	19				
Response 2: oxygen content (ANOVA for the 2FI model)						
Model	122.63	6	20.44	40.44	<0.0001	Significant
A: temperature	87.78	1	87.78	173.66	<0.0001	
B: pressure	3.64	1	3.64	7.20	0.0188	
C: time	9.30	1	9.30	18.40	0.0009	
AB	5.49	1	5.49	10.86	0.0058	
AC	1.23	1	1.23	2.43	0.1432	
BC	15.20	1	15.20	30.07	0.0001	
Residual	6.57	13	0.51			
Lack of fit	5.69	8	0.71	4.04	0.0703	Not significant
Pure error	0.88	5	0.18			
Cor total	129.21	19				

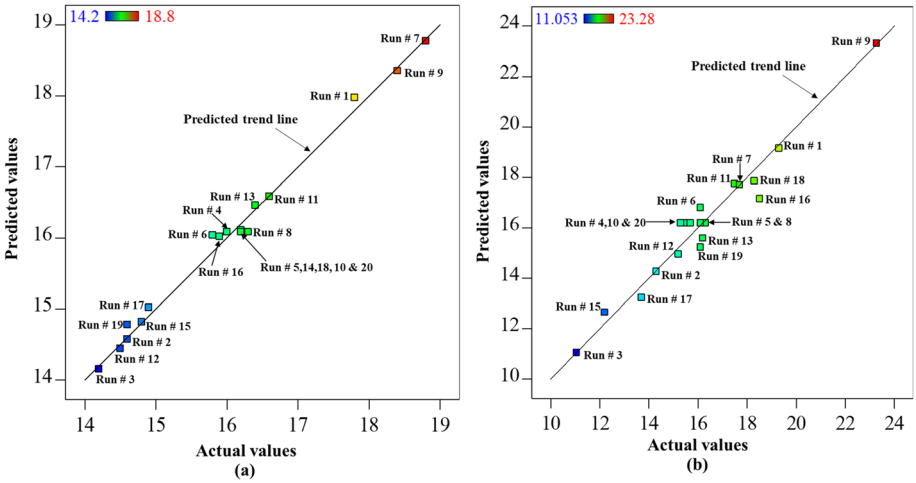

Fig. 3 Correspondence plot of the assessment between the predicted and actual experimental (a) biocrude yield and (b) oxygen content from all 20 hydrothermal liquefaction experimental runs of carrot wastes at 280–320 °C in 15–45 min. The color bar on the top left indicates the high (red) to low (blue) range of the experimental values of the biocrude yield and oxygen content in figures (a) and (b) respectively.

exhibited a significantly higher *F*-test value and a *p*-value less than 0.05, providing evidence to support the acceptability of the model. In addition, the *p*-value for each factor in the model (*p*-value < 0.05) indicates the level of confidence in the factor's contribution to the significance of the regression model.[35] The data shown provides compelling evidence that temperature significantly influences the yield of biocrude and oxygen content. This is supported by the *p*-value, which was determined to be less than 0.0001 for both factors. The aforementioned fact has been corroborated by the findings of our experimental study. The correlation between the experimental yield and anticipated yield of biocrude, as well as the oxygen content, was depicted in the parity plot (Fig. 3), demonstrating a reasonable level of agreement. The linear trend shown in the plot depicts the relationship between biocrude output and oxygen content. It is evident that, with the exception of a few experimental trials, the majority of the acquired outcomes are positioned either directly on or in close proximity to the projected trend line indicating that the model predicts experimental data reliably.

3.3. Variation of responses as per parameters

The regression model provides a comprehensive depiction of the impacts of many experimental factors, specifically process parameters, on the responses, namely biocrude yield and oxygen content. Furthermore, it elucidates the interplay among different variables and their influence on the outcome. The relevance of the factors mostly relies on the *p*-values associated with them, which should be below 0.05. According to the ANOVA table (Table 7), the factors of temperature (A), pressure (B), and time (C), as well as their respective squares (A^2, B^2, and C^2), exhibited *p*-values below 0.05. Notably, temperature emerged as the most influential factor.

Fig. 4 illustrates the impact of temperature, pressure, and duration on the production of biocrude. The data points

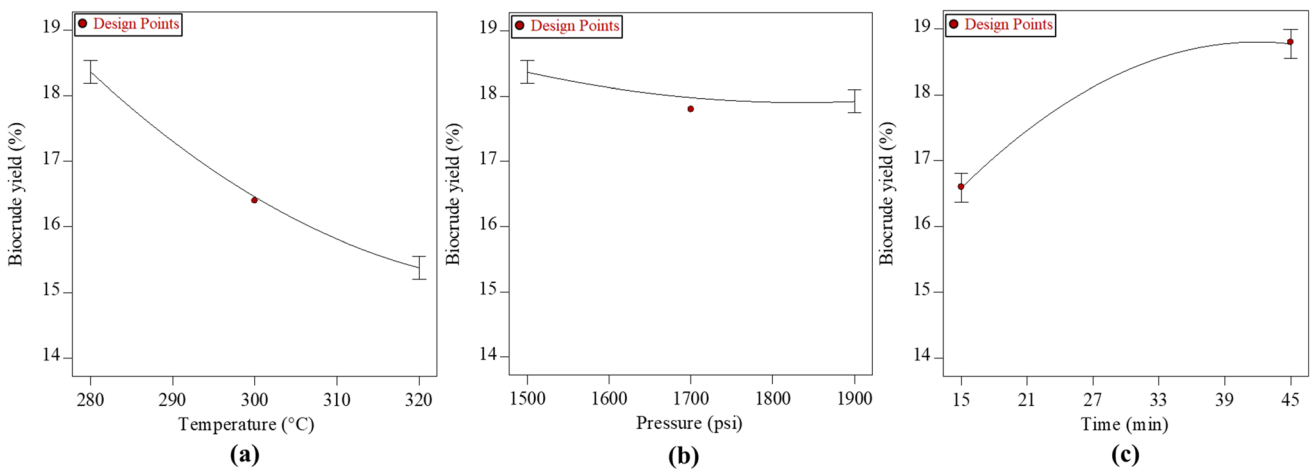

Fig. 4 Effects of (a) temperature at 1700 psi pressure, 30 min time; (b) pressure at 300 °C temperature, 30 min time; and (c) time at 300 °C temperature, 1700 psi pressure on biocrude yield.

depicted in Fig. 4(a) were obtained under varying temperatures ranging from 280 to 320 °C, while maintaining a constant pressure of 1700 psi and a fixed duration of 30 minutes. Based on the data presented in the figure, it can be observed that the biocrude yield exhibited an initial increase up to 18.8% at a specified temperature of 280 °C, beyond which a subsequent decline in yield was observed. This finding suggests that the impact of reaction temperature on the liberation of biomass macromolecules was more significant at lower temperatures compared to higher temperature circumstances. The potential cause of this phenomenon may be attributed to the relatively low concentration of solid particles present in the feedstock.[36] The decrease in biocrude yield with increase in temperature could be because of polymerization of the molecules to form solids, which justifies the high biochar yield with high temperature from Table 5. As per the literature, the biocrude yield from food waste increased with temperatures up to 300 °C and decreased with further increase in temperature due to decarbonylation, dehydration, and decarboxylation of the initially formed water-soluble molecules.[37] However, the pressure does not seem to affect the biocrude yield but the yield decreases slightly with increment in pressure as per Fig. 4(b). This may be due to the formation of more gaseous compounds with high pressure due to depolymerization. Similarly, Fig. 4(c) shows that the biocrude yield increases with increment in time; however, the yield is maximum (18.8%) at time of 42 minutes, and after that the yield is constant. The biocrude yield seemed to be increasing with reaction time at lower temperature than higher temperature. Similar results were also observed in the literature.[38] During the process of biomass hydrolysis, various intermediate byproducts such as ethers, esters, ketones, and aldehydes are formed. The extent to which these byproducts undergo depolymerization into chemicals (at higher temperatures) or polymerization into unwanted byproducts (at lower temperatures) tends to increase with longer reaction times.[39,40]

Fig. 5 represents the effects of temperature (*a*), pressure (*b*), and reaction time (*c*) on the oxygen content. It can be seen from the graphs that the temperature and pressure affect the oxygen content, while time does not. This could be due to the transfer of oxygen to aqueous and gaseous phases under higher temperature and pressure.

For easy understanding of the reader, Fig. 6 depicts the 2D and 3D contour plots demonstrating the collaborative impacts of temperature, pressure, and reaction time on the biocrude yield during HTL of food waste. It is perceptible from Fig. 6(a) and (d) that at a constant time with the temperature progress, the yield of biocrude reduced; however, with elevation of pressure it remains almost constant. The decrease in yield could be due to the polymerization of the molecules to form solids to form biochar at higher temperature, and depolymerization at higher pressure to form a gaseous product.[36] Similarly, in Fig. 6(b) and (e) the effect of time and temperature at a constant pressure of 1700 psi on the biocrude yield is shown. It is perceivable that with increasing time, the yield increases while it decreases with temperature elevation. This phenomenon may be attributed to the extended duration of reaction time, which enables the byproducts to undergo additional depolymerization into chemical compounds at elevated temperatures or polymerization into unwanted byproducts at lower temperature.[41,42] Similarly, Fig. 6(c) and (f) present the effects of time and pressure on the biocrude yield. It can be observed that the pressure did not affect the yield, however the yield increased with time. The impact of temperature and time on the yield is more pronounced compared to that of pressure.

In a similar way, Fig. 7 depicts the 2D and 3D contour plots representing the collaborative impacts of temperature, pressure, and reaction time on the oxygen content of the biocrude. The effects of pressure and temperature at a constant time of 30 min on the oxygen content are presented in Fig. 7(a) and (d). The oxygen content of the biocrude decreases with increase in temperature; this may be due to the production of more aqueous solution as the oxygenated compounds shift to the aqueous or gaseous phase at high temperature with time. However, there is a slight increase in oxygen content in the biocrude with increase in pressure. Fig. 7(b) and (e) show the effects of reaction time and temperature on the oxygen content.

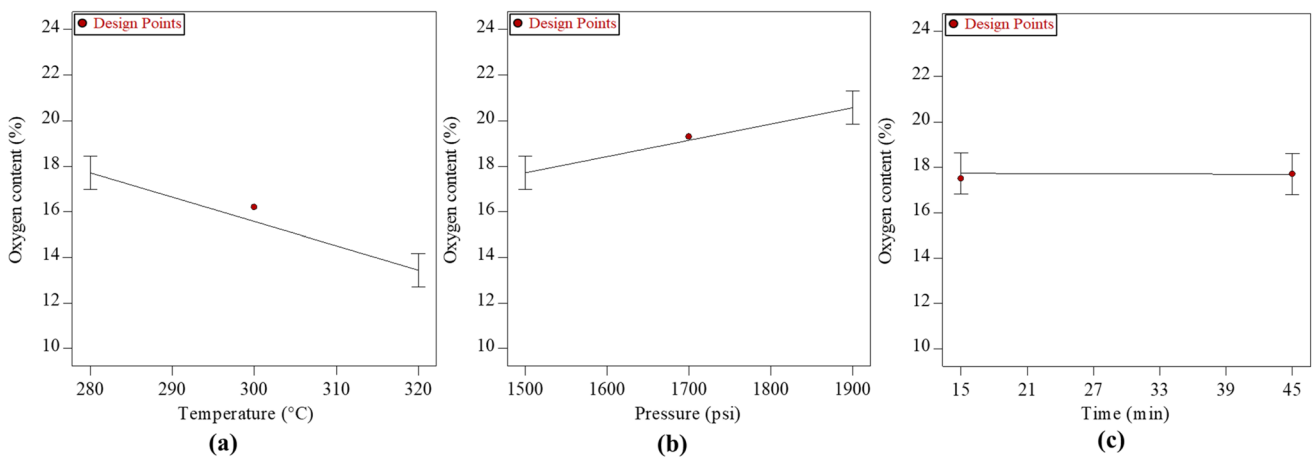

Fig. 5 Effects of (a) temperature at 1700 psi pressure, 30 min time; (b) pressure at 300 °C temperature, 30 min time; and (c) time at 300 °C temperature, 1700 psi pressure on oxygen content of the biocrude.

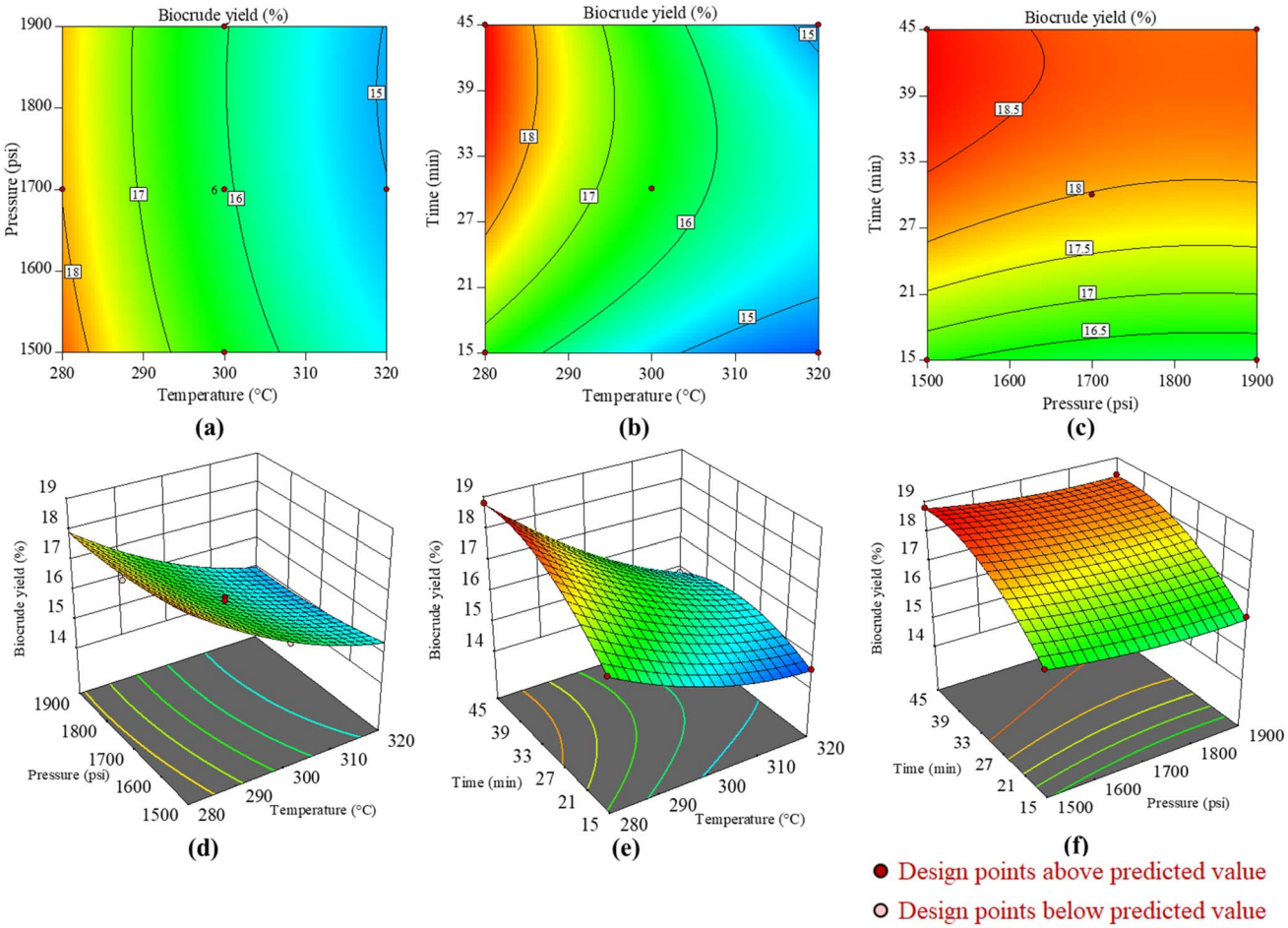

Fig. 6 (a)–(c) 2D contour plot and (d)–(f) 3D response surface plot showing the influence of reaction temperature and pressure, temperature and time, and pressure and time, respectively on biocrude yield from hydrothermal liquefaction of food waste.

It can be perceived that with an increase in time and temperature, the oxygen content decreases in the biocrude, maybe because of the shift of oxygenated compounds to the aqueous or gaseous phase. Similarly, Fig. 7(c) and (f) depict the combined effects of reaction time and pressure on the oxygen content of the biocrude. It can be observed that the increment of oxygen content with increment of time and pressure may be due to polymerization of the oxygenated compound at high pressure and time.[32] A similar type of result was also reported by Pattnaik *et al.*[32] for showing the effects of temperature and reaction time on total reducing sugar yields during subcritical water hydrolysis of phragmites.

Following the validation of the regression model utilizing multiple parameters, this study elucidates the interactions among distinct components and their respective effects on the yield of biocrude. The ultimate phase of the procedure was the retrieval of the optimization criteria from the statistical model that was built. The experimental study determined that the most favorable conditions for achieving the largest biocrude yields and minimizing the oxygen content during HTL of carrot waste were a temperature of 280 °C, a pressure of 1500 psi, and a reaction time of 42 minutes (Fig. 8). In addition to the optimized process conditions, the anticipated biocrude output and oxygen content were determined to be 18.8% and 17.7%, correspondingly. The biocrude yield was evaluated by conducting an optimization run with the implementation of these settings. The experimental error, as determined by the calculation using eqn (13), was observed to be 3.1%.

$$\text{Percent error } (\%) = \frac{\text{experimental value } (\%) - \text{predicted value } (\%)}{\text{experimental value } (\%)} \quad (13)$$

All the feedstocks undergo HTL under the optimized conditions and fitted with eqn (9) and (10) to verify the model. The biocrude yield, oxygen content, and their percent errors obtained from HTL of the feedstocks operated at optimum conditions (280 °C, 1500 psi, and 45 minutes) are shown in Table 8. As the errors are insignificant, it validates the model and establishes that it works for these food wastes.

3.4. Solvent optimization and quality analyses

By using optimized parameters, HTL experiments were carried out to optimize the solvent of filtration for yielding maximum

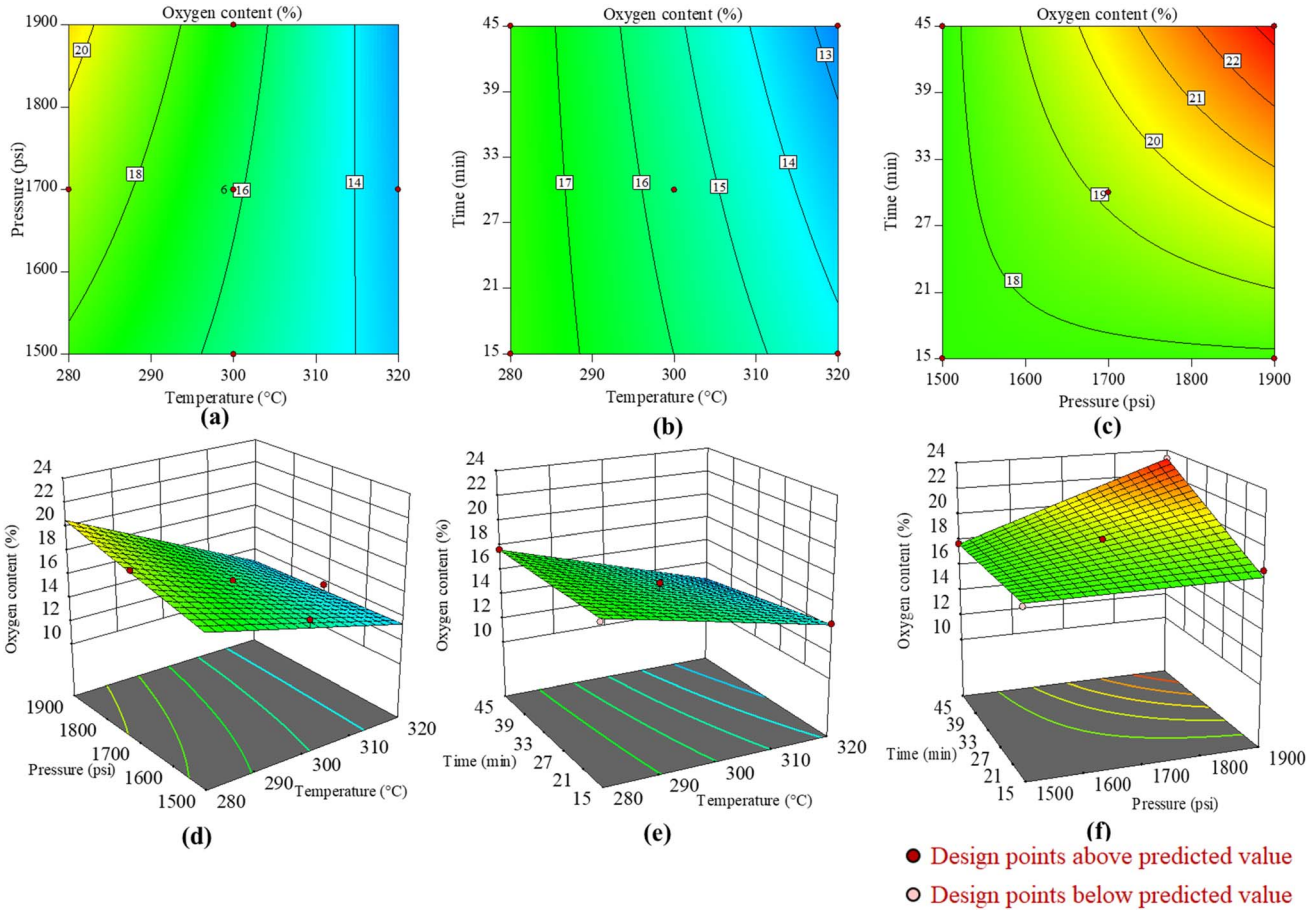

Fig. 7 (a)–(c) 2D contour plot and (d)–(f) 3D response surface plot showing the influence of reaction temperature and pressure, temperature and time, and pressure and time, respectively on oxygen content of the biocrude from hydrothermal liquefaction of food waste.

biocrude. For this purpose, solvents such as methanol, acetone, ethyl acetate, ethanol, dichloromethane, toluene, and hexane (Fisher Scientific, Edmonton, Canada) were selected. All the experiments were conducted in duplicate.

3.4.1. Higher heating values. Table 9 presents the biocrude yield from vacuum filtration with different solvents, their HHV, and elemental analysis. The best solvent was selected as per the highest biocrude yield, *i.e.*, methanol. It can be observed from the table that though the biocrude yield was highest for methanol, the oxygen content was high which is not desirable for a biocrude quality. Therefore, this process will further need upgradation to reduce the oxygen content to make desirable biocrude. The feedstock carrot waste has a HHV of 15.6 MJ kg^{-1}; the HHV for the subsequent biocrude has almost double the HHV value which shows the potential of the opted HTL of the food waste.

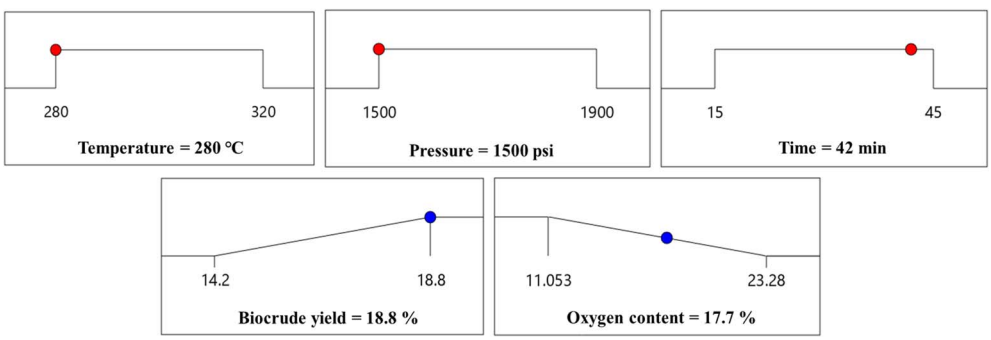

Fig. 8 Experimental boundaries set for each of the process parameters and the responses (biocrude yield and oxygen content) together with their optimum estimates.

Table 8 Biocrude yield, oxygen content, and their percent errors obtained from hydrothermal liquefaction of the feedstocks operated at optimum conditions (280 °C, 1500 psi, and 42 minutes)

	Biocrude		Oxygen content	
Feedstock	Yield (wt%)	Percent error (%)	Yield (wt%)	Percent error (%)
Beetroot	18.3	2.7	18.8	5.9
Brussels sprouts	17.9	5.0	19.5	9.2
Cabbage	18.2	3.3	18.4	3.8
Carrot	19.4	3.1	18.3	3.3
Celery	17.8	5.6	19.2	7.8
Corn	17.9	5.0	19.5	9.2
Onion	18.0	4.4	18.7	5.3
Parsnip	18.4	2.2	17.3	2.3
Pumpkin	17.9	5.0	18.8	5.9
Tomato	17.2	9.3	16.8	5.4

Table 9 Biocrude yield from filtration with different solvents and their ultimate analysis

Sl. no.	Solvents	Polarity index	Biocrude yield (wt%)	C (wt%)	H (wt%)	N (wt%)	S (wt%)	O (wt%)	HHV (MJ kg^{-1})	C recovery (%)	Viscosity (cP)
1	Methanol	5.1	19.6	70.0	7.8	1.4	0.2	20.7	30.8	55.9	1215
2	Acetone	5.1	18.8	73.5	7.2	1.3	0.3	17.7	31.3	63.7	1136
3	Ethyl acetate	4.4	18.6	74.4	7.7	1.4	0.1	16.5	32.1	65.7	1023
4	Ethanol	4.3	17.4	71.3	7.4	1.7	0.1	19.5	30.7	58.8	886
5	Dichloromethane	3.1	11.6	75.6	8.0	1.4	0.2	14.8	33.0	68.4	674
6	Toluene	2.4	10.2	77.6	8.4	1.0	0.2	12.8	36.4	72.8	515
7	Hexane	0.1	0	—	—	—	—	—	—	—	—

The results from Table 9 have shown that 55.9–72.8% of carbon has been recovered from carrot waste when it is converted to biocrude. A similar type of result has been reported for biocrude obtained from HTL of human feces by Lu *et al.*[43]

3.4.2. Thermogravimetric analysis. The thermogravimetric analysis (TGA) of carrot waste provides critical insights into its thermal degradation profile, which is essential for evaluating its potential for hydrothermal liquefaction (HTL), a promising method for converting biomass into bio-oil. The TGA results reveal a multi-stage decomposition pattern, highlighting its compositional diversity, including moisture, carbohydrates (cellulose and hemicellulose), lignin, proteins, lipids, and minerals. These findings are consistent with recent studies on biomass characterization and conversion pathways, which emphasize the role of thermal behavior in optimizing bioenergy processes.[44–46] In the initial temperature range below 150 °C, the weight loss of approximately 8–10% is primarily due to moisture evaporation. This phase is crucial for pre-drying considerations in HTL, as excessive moisture can influence the energy efficiency of the process.[46,47] Hydrothermal conditions (subcritical water environments) often eliminate the need for extensive pre-drying, leveraging the inherent moisture content of carrot waste for bio-oil production.[48]

In the temperature range of 200–350 °C, a significant weight loss of 50–55% is observed, dominated by the decomposition of hemicellulose and cellulose, along with contributions from proteins and lipids. This stage is pivotal for understanding the breakdown of macromolecules under hydrothermal conditions. In HTL, hemicellulose and cellulose hydrolyze into sugars and further degrade into smaller volatile compounds, which serve as precursors for bio-oil formation.[44,45,48] Proteins contribute to the nitrogen content in the resulting bio-crude, while lipids enhance the yield and quality of the oil fraction, aligning with previous findings on the role of biochemical composition in biomass liquefaction.[46–48] In the higher temperature range of 350–500 °C, a further weight loss of approximately 20–25% is observed. While this phase includes the thermal degradation of lignin, which accounts for 8.1% of the carrot waste, the remaining weight loss in this range is attributed to the slow decomposition of other components such as proteins, residual carbohydrates, and complex organic substances such as pectins and phenolic compounds. These components, though in smaller amounts, degrade over a broad temperature range and contribute to the overall weight loss. Additionally, any unconverted lipids and the more thermally resistant fractions of hemicellulose and cellulose might also degrade in this stage.[45,48,49] This phase underscores the complexity of carrot waste and its potential for producing bio-oil rich in diverse organic fractions, suitable for industrial applications.[46,49]

Above 500 °C, the residual material, representing 15–20% of the initial weight, consists of inorganic minerals and ash. The mineral content, including calcium, potassium, and other trace elements, is relevant for designing catalysts or addressing potential challenges such as fouling during HTL.[45,46,48] The

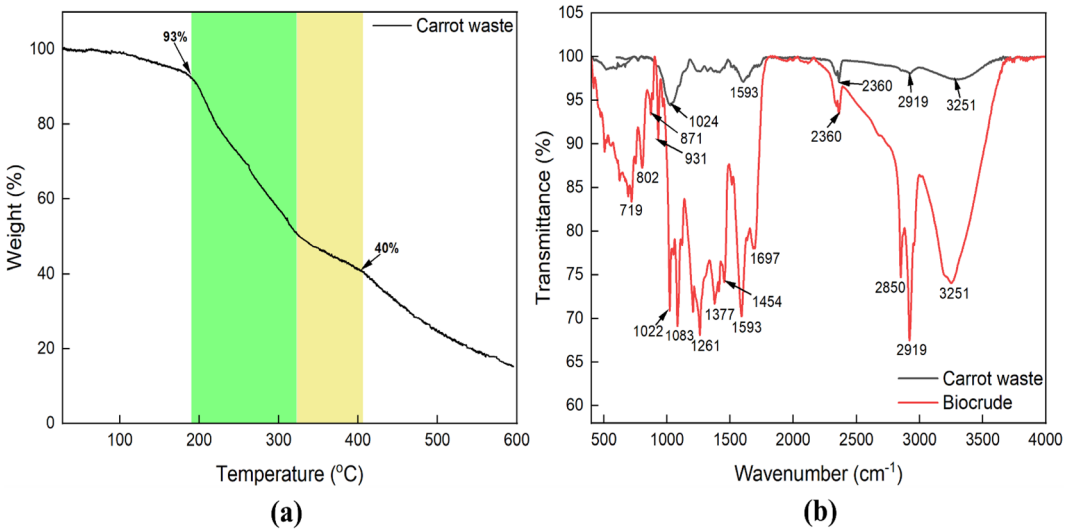

Fig. 9 (a) Thermal degradation properties of the raw feedstocks, (b) FTIR spectroscopy of feedstock and biocrude.

integration of TGA insights with HTL studies suggests that carrot waste's thermal characteristics make it a suitable feedstock for hydrothermal processing, offering a sustainable pathway for bioenergy and bioproducts.[46,49]

3.4.3. Chemical composition. The FTIR spectra of food waste and biocrude are shown in Fig. 9(b). In the biocrude, the bands at 3241, 2919, 2850, 2360, 1695, 1593, 1454, 1377, 1261, 1083, 1022, 931, and 871–719 cm^{-1} represented –OH stretching (carbohydrates, proteins, polyphenols), –CH stretching (aliphatic groups), –CH stretching (aliphatic groups), C=C stretching (alkenes), C=O stretching (esters, aldehydes, ketones, amides), C=C stretching (unsaturated compounds), –CH stretching (aliphatic bending groups), C–H deformation in CH_2 groups, C–O–C stretching (esters, ethers, other phenolic compounds), C–O stretching (carbohydrates), C–O (alcohols), C–H in plane benching (aromatic compounds), and –C=O bending (inorganic carbonates), respectively.[50,51] Similarly, the food waste bands at 3251, 2919, 2360, 1593, and 1024 cm^{-1} represented the O–H stretching (polymeric O–H, waster impurities), C–H stretching, (alkanes), C=C conjugated and C≡C stretching, C=C stretching (alkenes), and C–O stretching (primary, secondary, tertiary alcohol), respectively.[50,52]

3.4.4. Gas chromatography-mass spectrometry (GC-MS). The GC-MS analyzed chemical composition of biocrude obtained from filtration by different solvents is shown in Table 10. The components in the biocrude derived with methanol have more polar compounds; therefore it could be assumed that because of this reason, the crude had more viscosity (1215 cP) and the highest yield (19.6%). Similar results was also obtained for the biocrude derived with acetone. As we move down the table, the components obtained in the biocrude can be correlated with their polarity, viscosity, and yield. The components in biocrude derived with toluene have more hydrocarbons, are less viscous (515 cP) and non-polar, and therefore the biocrude had low yield (10.2%) compared to other biocrudes. The % composition in the Table represents the percentage of the respective compound present in the biocrude derived from the respective solvents. For example, in the biocrude derived from methanol that was analyzed by GC-MS, 4-(2-methoxyethyl)phenol content was 17.1%, and the rest of the % composition follows similarly.

The GC-MS results of biocrude obtained from HTL reveal a complex composition of hydrocarbons (for example, 1,5-heptadien-3-yne; ethylbenzene; 1,2,3,4-tetrahydro-1,1,6-trimethyl-naphthalene, *etc.*), carboxylic acids (9-hexadecenoic acid), ketones (1(3*H*)-isobenzofuranone), alcohols (phenol; 1,2-nonadecanediol), esters (isohexyl oxalic acid neopentyl ester); (2-methoxy-4-methyl-3-nitro-benzoic acid methyl ester), and other organic compounds as shown Table 10. The detailed GC-MS analysis allows for identifying specific biofuel components, aiding in optimizing HTL processes for enhanced bioenergy production from food waste. As seen from Table 10, many of the compounds that are absent in biocrude derived using DCM solvent are present in biocrude derived using methanol. This confirms that non-polar solvents like DCM extract them during distillation and leave the biocrude free from them.[53] It is also observed that the cyclic hydrocarbons (1,3-dimethyl-, *trans*-cyclohexane; cyclooctane), non-cyclic hydrocarbons (1,5-heptadien-3-yne; 1-undecene), and aromatic hydrocarbons (ethylbenzene; *p*-xylene) are the major groups in biocrude extracted using toluene, whereas phenolic derivatives (phenol; 4-(2-methoxyethyl)phenol), carboxylic acids/derivatives (2-hydroxy-5-nitro-benzoic acid); 9-hexadecenoic acid; phthalic acid ester derivatives, and other ester derivatives, ketones (1-(2-carboxy-4,4-dimethylcyclobutenyl, 1-buten-3-one)), alcohols (derivatized ribitol; 1,2-nonadecanediol), lower amount of hydrocarbons (1,1′-dodecylidenebis-4-methyl-benzene; 3,7-dimethyl-1-octene; 11-tricosene), and furanic compound (2-vinylfuran) are the main groups of biocrude recovered using methanol.[54,55] The product profiles for methanol, acetone, ethyl acetate, and ethanol are almost the same because of their comparable high polarity.[56] However, the major portion of acetone extracted biocrude contains 4-hydroxy-4-methyl-2-

Table 10 GC-MS analyzed composition of biocrude derived from filtration with different solvents

Retention time	Compound name	Formula	% composition
Methanol			
4.81	4-(2-Methoxyethyl)phenol	$C_9H_{12}O_2$	17.1
6.5	1-Buten-3-one, 1-(2-carboxy-4,4-dimethylcyclobutenyl)-	$C_{11}H_{14}O_3$	2.2
6.82	Ribitol, 1,3:2,4-di-*O*-benzylidene-	$C_{19}H_{20}O_5$	5.3
7.17	Benzoic acid, 2-hydroxy-5-nitro-	$C_7H_5NO_5$	0.9
7.53	Benzene, 1,1′-dodecylidenebis-4-methyl-	$C_{26}H_{38}$	1.1
7.99	Morpholine, 3-(4,5-dihydroxy)phenyl-	$C_{10}H_{13}NO_3$	3.9
8.79	Phenol	C_6H_6O	5.3
8.88	2-Vinylfuran	C_6H_6O	9.6
9.84	Oxirane-2-carboxylic acid, 3-(3,4,5-trimethoxyphenyl)-, methyl ester	$C_{13}H_{16}O_6$	0.2
10.08	Phthalic acid, 4-methoxyphenyl phenyl ester	$C_{21}H_{16}O_5$	0.9
10.42	1,2-Nonadecanediol	$C_{19}H_{40}O_2$	0.8
11.45	1-Octene, 3,7-dimethyl-	$C_{10}H_{20}$	1.5
11.6	1,3-Dioxane, 4-(hexadecyloxy)-2-pentadecyl-	$C_{35}H_{70}O_3$	0.1
13.39	9-Hexadecenoic acid	$C_{16}H_{30}O_2$	3.7
15.07	11-Tricosene	$C_{23}H_{46}$	1.6
17.5	Hexadecanoic acid, methyl ester	$C_{17}H_{34}O_2$	6.1
18.63	9-Octadecenoic acid (*Z*)-, methyl ester	$C_{19}H_{36}O_2$	3.8
18.78	Heptadecanoic acid, 16-methyl-, methyl ester	$C_{19}H_{38}O_2$	2.1
21.09	Phthalic acid, di(2-propylpentyl) ester	$C_{24}H_{38}O_4$	9.5
Acetone			
4.81	3-Penten-2-one, 4-methyl-	$C_6H_{10}O$	6.5
5.53	Oxalic acid, isohexyl neopentyl ester	$C_{13}H_{24}O_4$	0.8
5.75	1-Hexadecanol, 2-methyl-	$C_{17}H_{36}O$	0.5
5.9	Heptane, 3,5-dimethyl-	C_9H_{20}	3.6
6.1	2-Pentanone, 4-hydroxy-4-methyl-	$C_6H_{12}O_2$	49.9
6.43	Heptane, 2,4-dimethyl-	C_9H_{20}	4.1
6.49	Heptane, 3,4-dimethyl-	C_9H_{20}	1.8
6.62	Octane, 4-methyl-	C_9H_{20}	3.7
6.66	Octane, 2-methyl-	C_9H_{20}	1.6
6.75	Heptane, 3-ethyl-	C_9H_{20}	1.0
6.8	Heptane, 2,5-dimethyl-	C_9H_{20}	4.1
8.85	Phenol	C_6H_6O	17.0
10.29	Paromomycin	$C_{23}H_{45}N_5O_{14}$	1.3
Ethyl acetate			
8.86	Phenol	C_6H_6O	78.5
9.12	7-Oxabicyclo[4.1.0]heptane, 2-methylene-	$C_7H_{10}O$	2.6
10.3	Paromomycin	$C_{23}H_{45}N_5O_{14}$	6.7
12.35	Gibberellic acid	$C_{19}H_{22}O_6$	0.5
13.13	Naphthalene, 1,2,3,4-tetrahydro-1,1,6-trimethyl-	$C_{13}H_{18}$	2.7
Ethanol			
5.21	1(3*H*)-Isobenzofuranone	$C_8H_6O_2$	44.3
7.6	Benzoic acid, 2-methoxy-4-methyl-3-nitro-	$C_{10}H_{11}NO_5$	36.4
8.99	Benzoic acid, 4-(1,3-dioxolan-2-yl)-, methyl ester	$C_{11}H_{12}O_4$	3.5
9	Phenol	C_6H_6O	1.2
17.94	Hexadecanoic acid, ethyl ester	$C_{18}H_{36}O_2$	0.7
Dichloromethane			
8.83	Phenol	C_6H_6O	9.1
10.34	2,4-Heptadiene, 2,4-dimethyl-	C_9H_{16}	2.6
11.5	2(3*H*)-Naphthalenone, 4,4*a*,5,6,7,8-hexahydro-1-methoxy-	$C_{11}H_{16}O_2$	3.1
12.34	Phenol, 4-ethyl-2-methoxy-	$C_9H_{12}O_2$	5.6
13.14	Naphthalene, 1,2,3,4-tetrahydro-1,1,6-trimethyl-	$C_{13}H_{18}$	17.8
13.19	Ethanone, 1-(1-hydroxy-2,6,6-trimethyl-2,4-cyclohexadien-1-yl)-	$C_{11}H_{16}O_2$	1.9
Toluene			
7.43	1,5-Heptadien-3-yne	C_7H_8	49.8

Table 10 (*Contd.*)

Retention time	Compound name	Formula	% composition
7.5	1-Undecene	$C_{11}H_{22}$	1.1
7.54	Cyclohexane, 1,3-dimethyl-, *trans*-	C_8H_{16}	1.0
7.56	Cyclopentane, propyl-	C_8H_{16}	0.3
7.6	Cyclopentane, 1-ethyl-2-methyl-, *cis*-	C_8H_{16}	0.8
7.65	Cyclooctane	C_8H_{16}	1.5
7.67	Cyclohexane, ethyl-	C_8H_{16}	1.1
7.84	Ethylbenzene	C_8H_{10}	8.2
7.92	*p*-Xylene	C_8H_{10}	6.6

pentanone and phenol; ethyl acetate extracted biocrude contains phenol; and ethanol extracted biocrude contains 1(3*H*)-isobenzofuranone, and 2-methoxy-4-methyl-3-nitro-, methyl ester benzoic acid.[55]

3.4.5. Mineral compositions. The mineral composition was determined using an ICP-OES instrument. It was observed that the feedstock has a mineral composition of Na (1.04 wt%), Mg (0.41 wt%), K (5.23 wt%), and Ca (0.71 wt%), and the biocrudes extracted with solvents had the following mineral composition: methanol (0.98, 0.27, 5.05, 0.05 wt%), acetone (0.38, 0.02, 1.09, 0.05 wt%), ethyl acetate (0.44, 0.06, 0.93, 0.09 wt%), ethanol (0.61, 0.05, 2.21, 0.03 wt%), dichloromethane (0.25, 0.07, 1.30, 0.01 wt%), and toluene (0.07, 0.02, 0.35, 0 wt%), respectively. It was observed that the concentration of elements in the subsequent biocrudes has been reduced as predicted and there are no heavy metals detected for the desirable biofuel.[57] In summary, the examination of metal content indicated that the HTL process can be utilized as a promising method for extracting metals from biological waste, alongside the recovery of energy.[43]

4. Conclusions

This research has demonstrated the promising potential of valorizing food waste to produce biocrude. The reaction parameters were optimized at a temperature of 280 °C, pressure of 1500 psi, and reaction time of 42 minutes for treating wet samples. The R^2 value was 0.9. The independent variables in the design expert model were significant as $P \leq 0.05$. A higher F value suggested that the variables or model have a stronger statistical significance. The HTL process was proven to be efficient in breaking down complex organic molecules into a liquid fuel product (biocrude). The ultimate analysis of the biocrude showed C (70.0 wt%), H (7.8 wt%), N (1.4 wt%), S (0.2 wt%), and O (20.7 wt%) values. The oxygen content of the biocrude is high; however, it can be eliminated upon upgradation in future work, such as hydrodeoxygenation, catalytic cracking, decarboxylation, esterification, *etc.* The characterized biocrude exhibits properties that make it a viable candidate for blending with conventional fossil fuels or as a standalone transportation fuel. Its HHV (30.8 MJ kg^{-1}) is found to meet relevant standards and specifications for transportation fuel applications, with viscosity ranging from 515–1215 cP. This high viscosity is because it contains a high heteroatom content, mainly O and H, and this is the reason why it is more viscous at room temperature. Therefore, future work includes the biocrude to be upgraded in terms of hydrotreatment to be blended with conventional fuel for its use as a transportation fuel. Additionally, the biocrude obtained has 55.9–72.8% carbon recovery potential. The biocrude yield varies with the selection of solvents and their polarity. The solvents with higher polarity yield more biocrude. The use of biocrude derived from food waste can contribute significantly to reducing greenhouse gas emissions and dependence on finite fossil fuel resources. This aligns with the global sustainability goals of mitigating climate change and achieving a more circular economy. While the study has demonstrated significant progress, challenges such as scale-up, economic viability, and technology optimization remain to be studied. Future research should focus on addressing these challenges to facilitate the practical implementation of food waste-derived biocrude as a transportation fuel.

Data availability

The authors confirm that the data supporting the findings of this study are available within the article. Raw data that support the findings of this study are available from the corresponding author, upon reasonable request.

Author contributions

Kshanaprava Dhalsamant: conceptualization; data curation; formal analysis; investigation; methodology; project administration; resources, software, validation; writing – original draft; writing – review & editing. Ajay Kumar Dalai: funding acquisition, resources; supervision, writing – review & editing.

Conflicts of interest

The authors declare that they have no known competing financial interests or personal relationships that could have appeared to influence the work reported in this paper.

Acknowledgements

The authors acknowledge the funding from the Canada Research Chair (CRC) Program and Natural Sciences and Engineering Research Council of Canada (NSERC) for this research.

References

1 FAO, *Food and Agriculture Organizations of the United Nations*, **https://www.fao.org/platform-food-loss-waste/flw-data/en/**, accessed 19 October 2023.
2 StatCan, *Statistics Canada*, **https://www150.statcan.gc.ca/n1/en/subjects/agriculture_and_food/food**, accessed 19 October 2023.
3 US EPA, *Sustainable management of food basics*, United States Environ. Prot. Agency, 2015.
4 USDA, *Food Waste FAQs*, USDA, **https://www.usda.gov/foodwaste/faqs**.
5 K. Dhalsamant, P. Tirumareddy, V. B. Borugadda and A. K. Dalai, *Bioresour. Technol. Rep.*, 2023, **24**, 101595.
6 M. Govarthanan, S. Manikandan, R. Subbaiya, R. Y. Krishnan, S. Srinivasan, N. Karmegam and W. Kim, *Fuel*, 2022, **312**, 122928.
7 F. Pattnaik, S. Nanda, V. Kumar, S. Naik and A. K. Dalai, *Fuel*, 2022, **311**, 122618.
8 S. Jain, *Sustain. Energy Technol. Assessments*, 2023, **58**, 103380.
9 P. Ranganathan, *Sustain. Energy Technol. Assessments*, 2023, **57**, 103164.
10 R. Y. Krishnan, S. Manikandan, R. Subbaiya, W. Kim, N. Karmegam and M. Govarthanan, *Sustain. Energy Technol. Assessments*, 2022, **52**, 102211.
11 A. Aierzhati, M. J. Stablein, N. E. Wu, C. T. Kuo, B. Si, X. Kang and Y. Zhang, *Bioresour. Technol.*, 2019, **284**, 139–147.
12 S. Changi, M. Zhu and P. E. Savage, *ChemSusChem*, 2012, **5**, 1743–1757.
13 Y. Fan, U. Hornung, N. Dahmen and A. Kruse, *Biomass Convers. Biorefin.*, 2018, **8**, 909–923.
14 M. Pecchi, M. Baratieri, A. R. Maag and J. L. Goldfarb, *Waste Manage.*, 2023, **168**, 281–289.
15 S. Wainaina, M. K. Awasthi, S. Sarsaiya, H. Chen, E. Singh, A. Kumar, B. Ravindran, S. K. Awasthi, T. Liu, Y. Duan, S. Kumar, Z. Zhang and M. J. Taherzadeh, *Bioresour. Technol.*, 2020, **301**, 122778.
16 A. Le Pera, M. Sellaro, E. Bencivenni and F. D'Amico, *Waste Manage.*, 2022, **139**, 341–351.
17 W. M. L. K. Abeyratne, H. Bayat, H. M. K. Delanka-Pedige, Y. Zhang, C. E. Brewer and N. Nirmalakhandan, *J. Environ. Chem. Eng.*, 2023, **11**, 109628.
18 D. Yu, J. Guo, J. Meng and T. Sun, *Chemosphere*, 2023, **328**, 138606.
19 Z. X. Xu, J. H. Cheng, Z. X. He, Q. Wang, Y. W. Shao and X. Hu, *Bioresour. Technol.*, 2019, **278**, 311–317.
20 O. Fadele, I. N. A. Oguocha, A. G. Odeshi, M. Soleimani and L. G. Tabil, *Cellulose*, 2019, **26**, 9463–9482.
21 F. Pattnaik, S. Nanda, V. Kumar, S. Naik and A. K. Dalai, *Fuel*, 2022, **311**, 122618.
22 I. H. Cho and K. D. Zoh, *Dyes Pigm.*, 2007, **75**, 533–543.
23 A. Matayeva, D. Bianchi, S. Chiaberge, F. Cavani and F. Basile, *Fuel*, 2019, **240**, 169–178.
24 H. F. Khalekuzzaman, M. Fayshal and M. A. Adnan, *J. Cleaner Prod.*, 2024, **436**, 140593.
25 A. Mathanker, D. Pudasainee, A. Kumar and R. Gupta, *Fuel*, 2020, **271**, 117534.
26 P. W. Simon, A. Nijabat, S. Bibi, M. Ajmal, S. Nawaz, M. Z. Sajid, S. Ullah Khan Leghari, M. Mahmood-ur-Rehman, N. Huma Naveed and A. Ali, *Nat. Prod. Res.*, 2023, 1–10.
27 R. Ghadge, N. Nagwani, N. Saxena, S. Dasgupta and A. Sapre, *Energy Convers. Manage.:X*, 2022, **14**, 100223.
28 T. Shan Ahamed, S. Anto, T. Mathimani, K. Brindhadevi and A. Pugazhendhi, *Fuel*, 2021, **287**, 119329.
29 M. Mohan, R. Timung, N. N. Deshavath, T. Banerjee, V. V. Goud and V. V. Dasu, *RSC Adv.*, 2015, **5**, 103265–103275.
30 G. J. Swamy, A. Sangamithra and V. Chandrasekar, *Dyes Pigm.*, 2014, **111**, 64–74.
31 J. A. Okolie, S. Nanda, A. K. Dalai and J. A. Kozinski, *Int. J. Hydrogen Energy*, 2020, **45**, 18275–18288.
32 F. Pattnaik, S. Nanda, V. Kumar, S. Naik and A. K. Dalai, *Biomass Bioenergy*, 2021, **145**, 105965.
33 K. Manorach, A. Poonsrisawat, N. Viriya-Empikul and N. Laosiripojana, *Optimization of Sub-critical Water Pretreatment for Enzymatic Hydrolysis of Sugarcane Bagasse*, Elsevier B.V., 2015, vol. 79.
34 S. Masoumi and A. K. Dalai, *J. Cleaner Prod.*, 2020, **263**, 121427.
35 A. Purnomo, Y. A. W. Yudiantoro, J. N. Putro, A. T. Nugraha, W. Irawaty and S. Ismadji, *Int. J. Ind. Chem.*, 2016, **7**, 29–37.
36 J. Nallasivam, B. E. Eboibi, A. Isdepsky, M. Lavanya, S. Bhaskar and S. Chinnasamy, *Biomass Convers. Biorefin.*, 2022, **12**, 3827–3841.
37 B. Motavaf and P. E. Savage, *ACS ES&T Eng.*, 2021, **1**, 363–374.
38 B. Zhang, J. Chen, S. Kandasamy and Z. He, *Energy*, 2020, **193**, 116645.
39 G. Zhu, X. Zhu, Q. Fan and X. Wan, *J. Anal. Appl. Pyrolysis*, 2011, **90**, 182–186.
40 R. Lin, J. Cheng, L. Ding, W. Song, F. Qi, J. Zhou and K. Cen, *Bioresour. Technol.*, 2015, **186**, 8–14.
41 F. Bayat, S. Osfouri and R. Azin, *Biomass Bioenergy*, 2023, **178**, 106963.
42 Z. Zhu, L. Rosendahl, S. Sohail and G. Chen, *Sci. Total Environ.*, 2018, **630**, 560–569.
43 J. Lu, J. Zhang, Z. Zhu, Y. Zhang, Y. Zhao, R. Li, J. Watson, B. Li and Z. Liu, *Energy Convers. Manage.*, 2017, **134**, 340–346.
44 S. Elkhalifa, P. Parthasarathy, H. R. Mackey, T. Al-Ansari, O. Elhassan, S. Mansour and G. McKay, *Biomass Convers. Biorefin.*, 2022, 1–18.
45 J. S. Teh, Y. H. Teoh, H. G. How and F. Sher, *Processes*, 2021, **9**(9), 1610.
46 S. Elkhalifa, S. Mariyam, H. R. Mackey, T. Al-Ansari, G. McKay and P. Parthasarathy, *Energies*, 2022, **15**(17), 6277.

47 Y. S. Tanai, *Food Waste Energy Analysis: Characterizing Energy Content as a Function of Proximate Analysis Factors*, 2016, p. 2.
48 S. Mahadevan Subramanya and P. E. Savage, *ACS Sustain. Chem. Eng.*, 2021, **9**, 13874–13882.
49 J. Ni, L. Qian, Y. Wang, B. Zhang, H. Gu, Y. Hu and Q. Wang, *Fuel*, 2022, **327**, 125135.
50 M. Mecozzi, M. Pietroletti, M. Scarpiniti, R. Acquistucci and M. E. Conti, *Environ. Monit. Assess.*, 2012, **184**, 6025–6036.
51 X. Yang, H. Lyu, K. Chen, X. Zhu, S. Zhang and J. Chen, *BioResources*, 2014, **9**, 5219–5233.
52 C. Z. A. Ahmad, R. Hamidin, N. Ali and U. F. M. Abidin, *J. Mech. Eng. Sci.*, 2016, **7**, 1–23.
53 D. Xu and P. E. Savage, *Algal Res.*, 2014, **6**, 1–7.
54 H. Jahromi, T. Rahman, P. Roy and S. Adhikari, *Energy Convers. Manage.*, 2022, **263**, 115719.
55 J. Zhang and Y. Zhang, *Energy Fuels*, 2014, **28**, 5178–5183.
56 J. A. Joseph, S. Akkermans and J. F. M. Van Impe, *ACS Omega*, 2022, **7**, 24121–24133.
57 F. Naaz, A. Bhattacharya, K. K. Pant and A. Malik, *Process Saf. Environ. Prot.*, 2021, **145**, 141–149.